Wheel loader optimal transients in the short loading cycle

V. Nezhadali * **L. Eriksson** *

* *Electrical Engineering Department, Linköping University, SE-581 83 Linköping, Sweden (e-mail: {vaheed.nezhadali, lars.eriksson}@liu.se)*

Abstract: A nonlinear wheel loader model with nine states and four control inputs is utilized to study the fuel and time efficient optimal control of wheel loader operation in the short loading cycle. The wheel loader model consists of lifting, steering and powertrain subsystems where the nonlinearity originates from the torque converter in the drivetrain. The short loading cycle, from loading point to a load receiver and back to the loading point, for a fork lifting application is described in terms of boundary conditions of the optimization problem while the operation is divided into several phases with constant gearbox gear ratios in order to avoid discontinuities due to discrete gear ratios. The effect of load receiver standing orientation on the wheel loader trajectory, fuel consumption and cycle time is studied showing that a small deviation from the optimal orientation (≈ 20 [deg]) results in up to 18 % higher fuel consumption in the minimum time cycles. Also, an alternative lifting strategy where for operation safety load is lifted only when wheel loaders moves forward is studied showing that this increases the fuel consumption of a typical 25 [sec] cycle only less than 2 %. The wheel loader path between loading point and load receiver is also calculated by optimization and analyzed for different cases. It is shown that when the load receiver orientation is not optimized and is set manually, the time or fuel optimal paths will differ from the shortest distance path, however when the load receiver orientation is calculated by optimization the fuel, time and shortest distance paths become identical.

Keywords: Optimal control, switching control variable, nonlinear system, wheel loader, loading cycle

1. INTRODUCTION

Wheel loaders (WL) are widely used in mining and manufacturing operations as means to lift heavy materials up to desired positions. Fuel consumption and operational time of these vehicles affect the production cost and duration since loading operations performed by WLs are repetitive tasks. Developing efficient control systems and algorithms for WLs considering the operation time and fuel consumption is an interesting topic for manufacturers. Optimal control analysis of WL operation gives insights into available potentials for fuel consumption reduction without sacrificing the operation time. The sensitivity of WL transients with respect to various parameters can also be investigated via optimal control studies eliminating the need to perform costly experiments.

The current paper is a continuation of previous studies on modeling and control of a WL operating in lift-transport section of the short loading cycle. The novelty in this paper is that the optimization of WL operation is performed for the complete short loading cycle instead of only lifting-transport section which was carried out in Nezhadali and Eriksson (2014). The short loading cycle is one of the frequent applications of WLs and the schematic of this cycle is illustrated in Figure 1. The loading operation starts with lifting of the load from ground level (point 0) and moving backwards to the reversing point shown on the figure and then moving forward to point 4 where WL moves straight for L_p meters in order to avoid collision

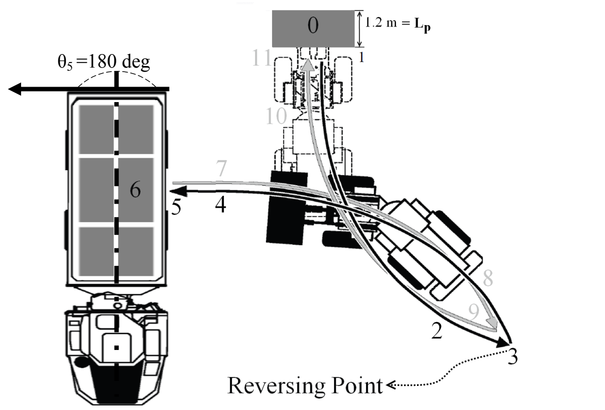

Fig. 1. Numbered sequence of actions in a short loading cycle where the load receiver orientation is $\theta_5 = 180$ [deg], picture from Filla (2011).

with pallets already loaded on the load receiver. At point 5 the WL stops, lowers the load and places it on load receiver's deck (point 6), and then moves back to the initial loading position (point 0) respectively.

In order to avoid damages to the mechanical structure of the WL, loading and unloading operations must be performed while WL is perpendicular to the load and load receiver respectively, Sarata et al. (2005). Therefore the orientation of the load receiver affects the trajectory of the

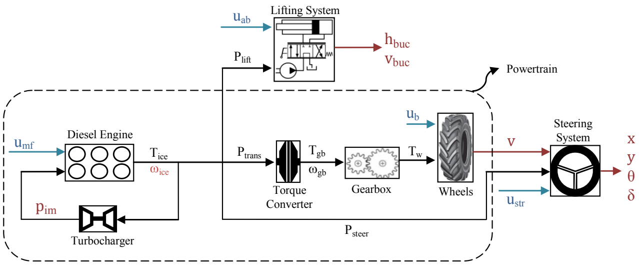

Fig. 2. Structure of the wheel loader model, components as well as the connection between them (system states in red, control inputs in blue and other parameters in black).

WL during the loading cycle. In Nezhadali et al. (2013), Nezhadali and Eriksson (2013) and Nezhadali and Eriksson (2014) it is investigated how the system transients, WL trajectory in the loading cycle, fuel consumption and cycle time get affected for cases where the load receiver orientation is set as a design variable in optimization and also where a fixed value is set as the desired orientation of the load receiver.

The other study in this paper focuses on the lifting operation. For safety reasons and in order to maintain the stability of the WL as well as not blocking the view of the WL operator while the load is being transferred, it is desirable to hold the load at low height and postpone lifting to the later periods of the cycle. To analyze the effects of such lifting strategies on system transients, fuel consumption and cycle time, the fuel and time efficient WL operations are analyzed for two cases where once the lifting can be performed freely during the whole cycle duration and in another lifting is allowed only in the part of the loading cycle where the WL moves forward to the load receiver. In all cases, the load is assumed to be a pallet with constant mass.

Considering the dimensions of the optimal control problem (OCP) formulated for the calculation of minimum fuel ($\min M_f$) or minimum time ($\min T$) transients in terms of number of states and control variable, loading cycle constraints at certain instances of the operation and the discontinuity of the gearbox gear ratios, solving the problem with methods such as Pontryagins Maximum Principle or Dynamic Programming is not feasible. Instead, as in Sivertsson and Eriksson (2013), an optimal control solver engine named PROPT TOMLAB (2012) is used where pseudospectral collocation method and SNOPT Gill et al. (1997) are used to discretize and solve the OCP respectively.

2. WHEEL LOADER SYSTEM MODEL

The model is the same as the one developed in Nezhadali and Eriksson (2014) where the WL is described as a nonlinear system composed of three main subsystems namely powertrain, lifting and steering as depicted in Figure 2. The nonlinearity in the WL model originates from the characteristics of the torque converter which is a function of wheel and engine speed ratio. A simplified version of the mean value diesel engine model in Eriksson (2007) produces the power required for lifting P_{lift}, steering P_{steer} and traction P_{trans} of the vehicle. The nine states of the model are engine speed ω_{ice}, intake manifold pressure p_{im}, vehicle speed v, vertical lifting speed v_{lift}, pallet height h_{lift}, vehicle positions in xy plane, vehicle heading angle θ and steering angle δ. The control inputs are fuel injection per combustion cycle of engine u_{mf}, bucket vertical acceleration u_{ab}, braking torque signal u_b, derivative of steering angle u_{dstr} and gear ratio in gearbox γ which is an integer. The governing differential equations in the model are:

$$\frac{d\omega_{ice}}{dt} = \frac{1}{J_{ice}}\left(T_{ice} - \frac{P_{lift} + P_{steer} + P_{trans}(\gamma)}{\omega_{ice}}\right) \quad (1)$$

$$\frac{dh_{lift}}{dt} = v_{lift} \quad (2)$$

$$\frac{dv_{lift}}{dt} = u_{ab} \quad (3)$$

$$\frac{dv}{dt} = \frac{sign(v)(F_{trac} - F_{roll})}{M_{tot}} \quad (4)$$

$$\frac{dp_{im}}{dt} = \frac{1}{\tau(\omega_{ice})}(p_{i,model}(\omega_{ice}, T_{ice}) - p_{im}) \quad (5)$$

$$\frac{d\theta}{dt} = \frac{v}{R(\delta)} \quad (6)$$

$$\frac{dx}{dt} = v\cos(\theta) \quad (7)$$

$$\frac{dy}{dt} = v\sin(\theta) \quad (8)$$

$$\frac{d\delta}{dt} = u_{dstr} \quad (9)$$

where τ and $p_{i,model}$ are respectively a time constant and static model of the intake manifold pressure model, T_{ice} is the engine output torque, M_{tot}, F_{trac} and F_{roll} are mass of loaded vehicle, tractive force and rolling resistance force, and finally R in (6) is the turning radius of the WL.

3. PROBLEM FORMULATION

The model described in the previous section is utilized to formulate OCPs for optimization of loading cycle duration or fuel consumption. There are different requirements at certain stages of the loading cycle and also the integer gear ratios (γ) impose discontinuities into the problem. To account for this discrete nature of the problem, the problem of finding $\min M_f$ or $\min T$ transients during the loading cycle is divided into several phases where the gear ratio remains constant during each phase and the phase duration is optimized. This is a common approach in nonlinear optimal control when there exist a switching control variable in the system, Sager (2009). As illustrated in Figure 1, the course of events in the loading cycle initiates at point 0 where $(x, y) = [0, 0]$ and continues as follows

- 0-1, Initial lifting of load from ground level to 20 [cm], WL is standing still at $(x, y) = [0, 0]$, $\gamma = 0$.
- 1-2, Lifting, steering and moving backwards, $\gamma = -60$.
- 2-3, Lifting, steering and moving backwards, braking to stop at reversing point, $\gamma = 0$.
- 3-4, Lifting, steering and moving forward, $\gamma = 60$, end height of the load achieved at $t = t_4$.
- 4-5, Moving straight for L_p [m] to place the pallet on the load receiver, braking, $\gamma = 0$.

- 5-6, Lowering the pallet 20 [cm] and placing it on load receiver's deck, WL stands still at $(x_e,\, y_e)$, $\gamma = 0$.
- 6-7, No lifting, moving L_p [m] backward to avoid collision between forks and the pallet, $\gamma = -60$.
- 7-8, Lowering the forks to 20 [cm] for safer operation, moving backward, $\gamma = -60$.
- 8-9, Braking to stop at reversing point, $\gamma = 0$.
- 9-10, Moving forward to the initial point, $\gamma = 60$.
- 10-11, Lowering the forks to ground level, braking to stop at $(x, y) = [0, 0]$, $\gamma = 0$.

where the second digits at the beginning of each item denote the phase number, i.e 0-1 is phase one, and $(x_e,\, y_e)$ is the desired position of the load receiver where the load should be transfered to. The gear ratio is set to 0 during braking, -60 while reversing and 60 when moving forward as suggested in Volvo (2012). The state and continuous control vectors s and u respectively read as

$$s := \left(\omega_{ice}\,, h_{lift}\,, v_{lift}\,, v\,, p_{im}\,, \theta\,, x\,, y\,, \delta\right)^T \tag{10a}$$

$$u := \left(u_{mf}\,, u_{ab}\,, u_b\,, u_{dstr}\right)^T \tag{10b}$$

Representing the system of ODEs in (1)-(9) by $\dot{s}(t) = f(s(t), u(t), \gamma(t))$, the $\min T$ and $\min M_f$ OCPs, time varying constraints and different phase requirements for $t \in [0, T]$ become

$$\min_{s(t),u(t),\gamma(t)} \quad T \quad \text{or} \quad M_f \tag{11a}$$

$$\begin{aligned}
&\text{s.t.}\\
&\dot{s}(t) = f(s(t), u(t), \gamma(t))\\
&u_{min} \le u(t) \le u_{max}\\
&s_{min} \le s(t) \le s_{max}\\
&R \le R_{max}\\
&T_{ice}(s(t), u(t)) \le T_{ice,max}\\
&s(0) = \left(120, 0, 0, 0, 1.1 \times 101300, \frac{\pi}{2}, 0, 0, 0\right)\\
t \in [0, t_1]:\ &\gamma(t) = 0, h_{lift}(t_1) = 0.2,\\
t \in [t_1, t_2]:\ &\gamma(t) = -60,\\
t \in [t_2, t_3]:\ &\gamma(t) = 0, v(t_3) = 0, \dot{v}_{min} \le |\dot{v}(t)|,\\
t \in [t_3, t_4]:\ &\gamma(t) = 60, h_{lift}(t_4) = h_{end},\\
t \in [t_4, t_5]:\ &\gamma(t) = 0, u_{dstr}(t) = u_{ab}(t) = \delta(t) = v(t_5) = 0,\\
&\int_{t_4}^{t_5} v\,\mathrm{d}t = L_p, (x, y)(t_5) = [x_e, y_e], \dot{v}_{min} \le |\dot{v}(t)|,\\
t \in [t_5, t_6]:\ &\gamma(t) = v(t) = 0, h(t_6) = h_{end} - 0.2,\\
t \in [t_6, t_7]:\ &\gamma(t) = -60, u_{ab}(t) = u_{dstr}(t) = \delta(t) = 0,\\
&\int_{t_6}^{t_7} v\,\mathrm{d}t = -L_p,\\
t \in [t_7, t_8]:\ &\gamma(t) = -60, h_{lift}(t_8) = 0.2,\\
t \in [t_8, t_9]:\ &\gamma(t) = 0, u_{ab}(t) = v(t_9) = 0, \dot{v}_{min} \le |\dot{v}(t)|,\\
t \in [t_9, t_{10}]:\ &\gamma(t) = 60, u_{ab}(t) = 0,\\
t \in [t_{10}, T]:\ &\gamma(t) = 0, u_{ab}(T) = u_{dstr}(T) = u_b(T) = 0,\\
&s(T) = \left(\text{-}, 0, 0, 0, \text{-}, \text{-}, 0, 0, 0\right), \dot{v}_{min} \le |\dot{v}(t)|,
\end{aligned} \tag{11b}$$

where L_p is the length of pallet holding the load and h_{end} is the desired load height at load receiver. The minimum and maximum limits applied on controls and states are due to component limitations and operating range. Vehicle deceleration during braking is limited by $\dot{v}_{min}$ in order to avoid harsh braking which may lead to vehicle instability if violated. The fuel consumption M_f in (11a) is calculated as the sum of fuel consumptions in all phases as follows

$$M_f = \int_0^{t_1} \dot{m}_f(s(t), u(t), \gamma(t))\,\mathrm{d}t + \\ \ldots + \int_{t_{10}}^{T} \dot{m}_f(s(t), u(t), \gamma(t))\,\mathrm{d}t \tag{12}$$

In order to ensure that speed and position states reach zero values at stationary, the values of their derivative (u_{dstr}, u_{ab}) is set to zero where it is applicable. In addition to the constraints stated in (11b) the states and control variables are ensured to be continuous between successive phases by applying the following constraint in the optimal control solver

$$(s_i, u_k)|_{\text{start of phase j+1}} = (s_i, u_k)|_{\text{ at end of phase j}} \\ i \in \{1, 2, ..., 9\},\, k \in \{1, 2, 3, 4\},\, j \in \{1, 2, ..., 10\} \tag{13}$$

Solving the OCP in (11a) w.r.t the constraints stated in (11b) results in oscillatory transients and control inputs which are attenuated by using the technique explained in Nezhadali and Eriksson (2013).

4. OPTIMIZATION RESULTS

The OCPs in (11a) with the constraints in (11b) and (13) are solved and the system transients are calculated and analyzed for three different cases. Once the optimal transients are calculated where load receiver orientation angle at point 6 of the loading cycle (see Figure 1), is calculated by the optimization, and another case where the orientation of the load receiver is fixed to $\theta_5 = \frac{\pi}{2}$ at t=T in (11b). The third case is the analysis of $\min T$ and $\min M_f$ transients when lifting is delayed to the intervals of the cycle where the vehicle moves towards the load receiver (between points 3 and 4 in Figure 1). Trade-offs between fuel consumption and cycle time, and the optimal path between point 0 and 11 of the cycle are compared for different cases. In order to compute each trade-off, the objective function in (11a) is reformulated as follows

$$\min_{s(t),u(t),\gamma(t)} \quad w_1 \times T + w_2 \times M_f \tag{14}$$

where w_1 and w_2 are weights with their sum equal to one and the problem is solved for various weights.

4.1 Sensitivity to the load receiver orientation

Trade-off between cycle time and fuel consumption

Figure 3 shows the trade-off between fuel consumption and cycle duration once for $\theta_5 = 180$ [deg] and another where $\theta_5 =$ free and thus calculated during min T/min M_f optimization. The fuel consumption in $\min M_f$ and cycle time in $\min T$ solutions increase when the orientation at unloading point is constrained while the increase in fuel consumption is higher in case of faster cycles. The higher fuel consumption in the shorter cycles is on one hand due to longer steering angle dynamics (longer intervals of $u_{dstr} \neq 0$) which leads to higher power consumption in the steering system ($P_{steer} = f(u^2_{dstr})$), and on the other hand, because the traveling distance increases up to 4.9 % at all

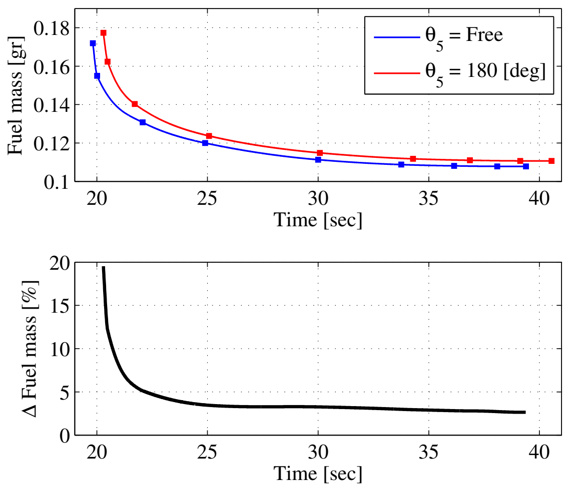

Fig. 3. Trade-off between fuel consumption and cycle time. Fuel consumption increases in all cycles when $\theta_5 = 180$ [deg].

cycle durations which increases the fuel consumption yet more. As the loading cycles get longer, there is less need to rapid changes in the steering angle and the required power for steering gets smaller leading to less increase in fuel consumption.

System transients in $\min T$ *and* $\min M_f$ *solutions*

Figure 4 shows the $\min T$ system transients for $\theta_5 =$ Free and $\theta_5 = 180$ [deg] respectively. While the major differences in the transients lie in the steering control input and state variables, the rest of transients are closely similar. In both cases, when the vehicle starts from stand still, first engine is accelerated up near to its maximum speed so that large torques become available at the torque converter output for faster vehicle acceleration. Load lifting starts a bit later in the second phase after the vehicle has reached high speed and less power is required for vehicle acceleration. The engine speed remains high so that a faster start is facilitated at the beginning of phase 4. The lifting speed peaks at the end of the third phase and the bucket speed starts reducing ($P_{lift} = 0$) at the same time as the WL starts from stand still at point 3 of the cycle. This leads to the same effect as that at the beginning of the second phase where engine power is fully allocated to faster vehicle acceleration by not lifting the load. As the WL approaches the load receiver late in the fourth phase, fuel injection is cut off and the engine inertia is used for traveling the rest of the distance up to the stopping point. While the load is lowered to be placed on the load receiver's deck (between ≈ 9.5 to 10.5 [s]), the engine is again accelerated in order to reach high speed before the WL starts to move backwards. During the return from load receiver to the initial point while WL is not loaded any longer, the engine is controlled such that engine speed is high at the start of the move from stand still and then engine deceleration takes place. Due to lower weight of the vehicle in this section of the cycle, intake manifold pressure is lower since intake manifold pressure is a function of both engine speed and load (T_{ice}).

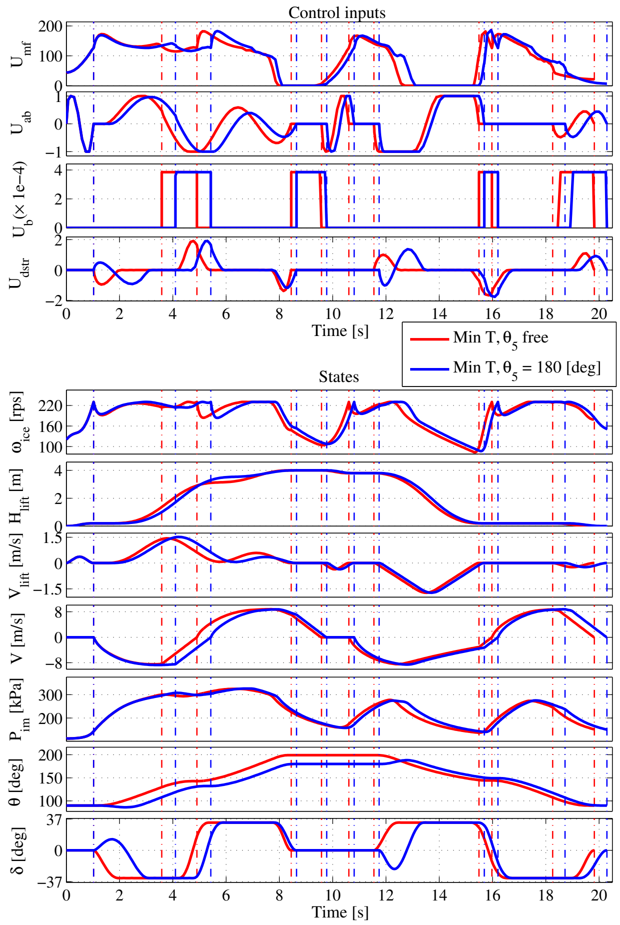

Fig. 4. $\min T$ controls and states for fixed and free θ_5. The dash-dotted lines are phase boundaries.

The fuel optimal transients for both θ_5 alternatives are illustrated in Figure 5. The transients in both cases are similar to those of the $\min T$ solution the difference being that the dynamics are stretched over a longer time interval while the major difference in the system transients between $\theta_5 = 180$ [deg] and θ_5=Free cases is observed to be the steering control input and states. Lifting starts almost from the middle of the second phase and intake manifold pressure is lower when returning from the load receiver towards initial loading point. Engine operates at lower speed compared to the $\min T$ transients which as discussed in Nezhadali et al. (2013) reduces the torque converter losses and increases the fuel efficiency.

4.2 Sensitivity to the lifting pattern

Trade-off between cycle time and fuel consumption

Delayed lifting strategy is applied for both fixed and free θ_5 and the trade-off between cycle time and fuel consumption is calculated using different weights in (14) as illustrated in Figure 6. Fuel consumption increases when lifting is delayed and the increase is larger in the shorter cycles rapidly vanishing as the cycle duration increases. The fact that a typical short loading cycle operation is performed in durations longer than that of the time optimal solution (around 25 [s] according to Nilsson et al. (2013)), reduces the importance of much higher fuel consumption near the $\min T$ solution.

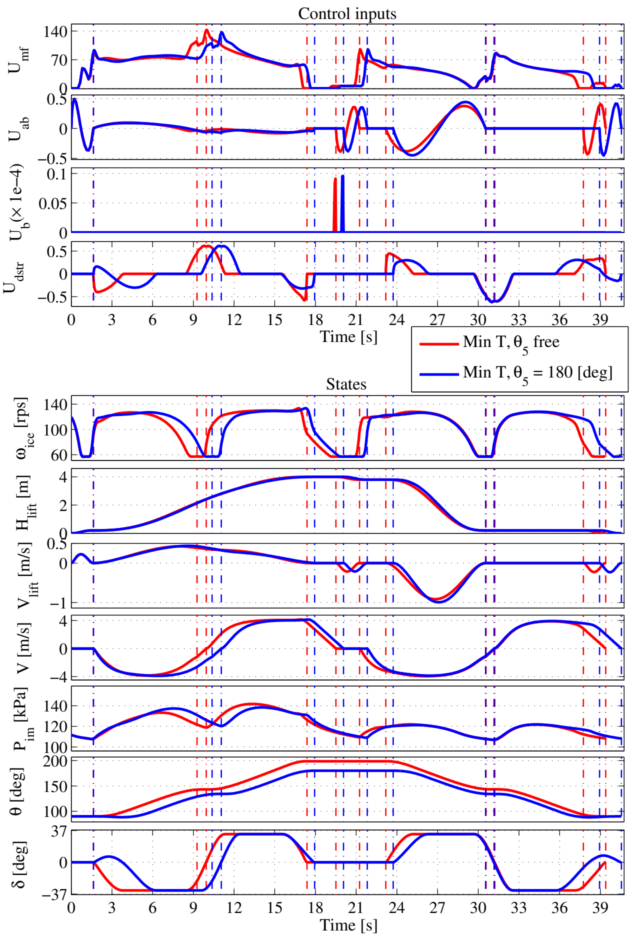

Fig. 5. $\min M_f$ controls and states for fixed and free θ_5. The dash-dotted lines are phase boundaries.

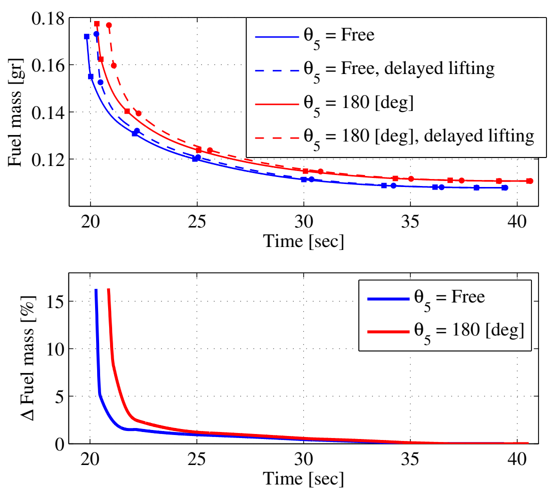

Fig. 6. Comparison of the trade-off between fuel consumption and cycle time for cycles with delayed lifting and normal cycles in case of free and fixed θ_5.

$\min T$ transients

Figure 7 shows the $\min T$ transients of the WL with free θ_5 for normal and delayed lifting. When lifting is delayed by setting $u_{dstr} = 0$ during the second and third phases, apart from changes in the lift speed, height and acceleration, engine speed and intake manifold pressure are also affected. Since larger torque is available at lower engine speed which increases the amount of generated power by the diesel engine, the engine is controlled such that it operates at lower speed during the fourth phase where a high power is demanded for both lifting and traction. The fact that less engine power is available for vehicle traction reduces the WL speed during the fourth phase thus increasing the duration of the $\min T$ transients when lifting is delayed.

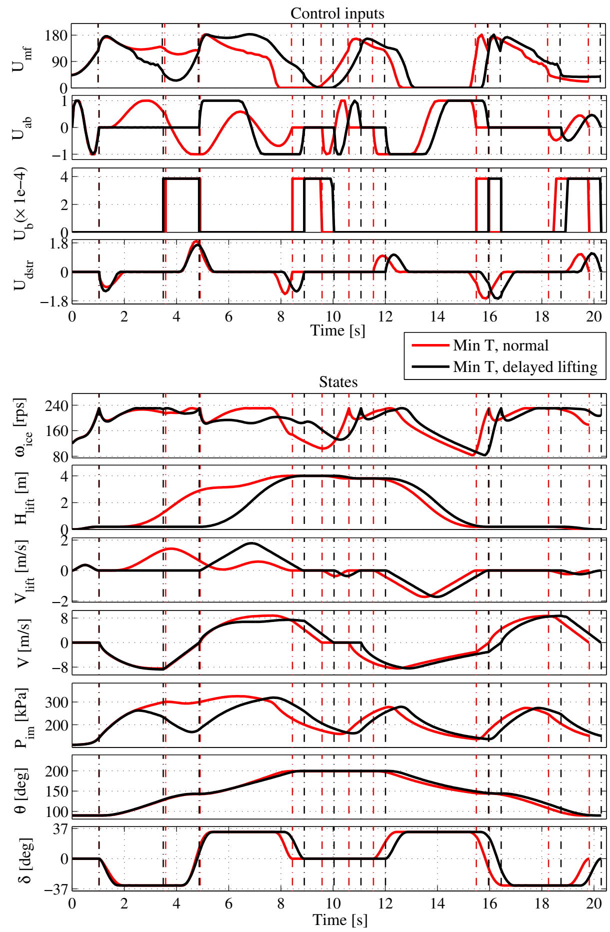

Fig. 7. $\min T$ controls and states for a normal cycle VS a cycle with delayed lifting, free θ_5. The dash-dotted lines are phase boundaries.

WL trajectory in $\min T$ and $\min M_f$ solutions

Figure 8 shows the WL path in the short loading cycle for $\min T$ and $\min M_f$ of normal and delayed lifting alternatives. The first observation is that the $\min T$ and $\min M_f$ trajectories are the same when there is no constraint on the orientation at point 5 of the cycle($\theta_5 =$ Free), and nothing changes when lifting is delayed, see Figure 8 left column. The WL is steered such that the path with shortest possible distance is selected in $\min T$ cycle which is the same as that of the $\min M_f$ cycle. The fact that the trajectories remain the same for both $\min T$ and $\min M_f$ cycle shows that the shortest path is unique and there is no alternative to travel the same distance in a shorter time or with lower fuel consumption.

On the other hand, when $\theta_5 = 180$ [deg], the $\min T$ and $\min M_f$ trajectories are not identical, see Figure 8 right column. Although the trajectories look different the distance traveled during the operation is identical

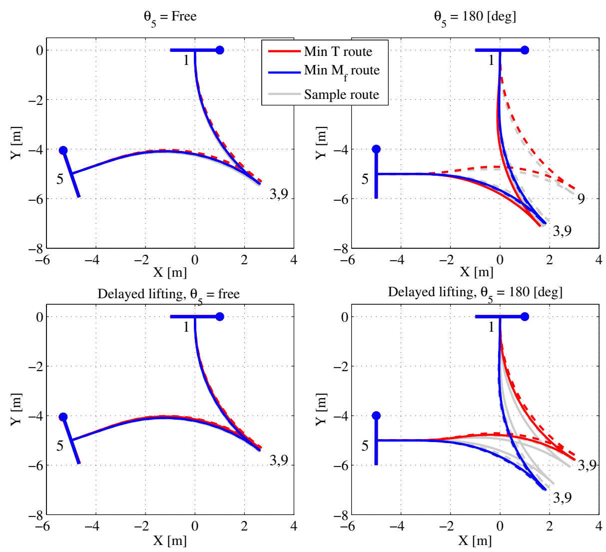

Fig. 8. Wheel loader optimal path for different cycles. The path from loading point 1 to the load receiver 5 is shown with solid line, and from 5 to starting point 1 with dashed line.

for both cases meaning that the trajectory with the shortest traveling distance is not unique and there exists an alternative where the same distance can be traveled in a shorter time ($\min T$ trajectory). However considering the power required for steering in any of the two trajectories, $\min T$ trajectory requires more steering power compared to the $\min M_f$ trajectory. Therefore, when fuel consumption becomes a part of the objective function in the OCP ($w_2 \neq 0$ in (14)), the trajectory with the lower steering power consumption is selected while the traveling distance remains unchanged.

5. CONCLUSION

The fuel and time efficient controls of a wheel loader operating in short loading cycle is calculated and analyzed by solving optimal control problems. A nonlinear wheel loader model with nine states and four control inputs is used, and the complete loading cycle starting by initial load lifting from ground level until the wheel loader places the load on the deck of a load receiver and the way back to the initial point is described in the problem formulation. In order to include discrete gear ratios of the gearbox in the problem formulation without facing discontinuities, the problem is divided into several phases during which the gear ratio remains constant.

The sensitivity of the minimum fuel and minimum time transients to the angle in which the wheel loader meets the load receiver is analyzed by calculating the trade-off between fuel consumption and cycle time duration for two cases where in one the orientation angle is calculated by the optimization, and in another it is set as a fixed parameter. The results show that in typical short loading cycles with 25 [s] duration, the fuel consumption increases up to 4 % when the load receiver orientation deviates from the optimal.

In another case, an alternative lifting strategy where load lifting is limited to the period of the cycle that the wheel loader moves forward is studied. This is a common practice in wheel loader operation in order to increase safety. Calculating the trade-off again, it is shown that in this case, the increase in the fuel consumption of a typical short loading cycle operation is less than 2 %.

The wheel loader path in the short loading cycle is also analyzed for the different cases showing that the shortest path is unique and identical for the minimum fuel and minimum time operations when the load receiver orientation is optimized but in case of a slightly perturbed from optimal load receiver orientation angle, the shortest path with minimum traveling distance between loading point and the load receiver is not unique and alternatives with lower fuel consumption or operational time exist.

REFERENCES

Eriksson, L. (2007). Modeling and control of turbocharged SI and DI engines. *Oil & Gas Sicence and Technology Rev. IFP*, 523–538.

Filla, R. (2011). *Quantifying Operability of Working Machines*. Ph.D. thesis, Linköping University, Dissertation, NO. 1390.

Gill, P.E., Murray, W., Michael, and Saunders, A. (1997). An sqp algorithm for large-scale constrained optimization. *SIAM Journal on Optimization*.

Nezhadali, V. and Eriksson, L. (2013). Optimal control of wheel loader operation in the short loading cycle using two braking alternatives. In *IEEE VPPC 2013 – The 9th IEEE Vehicle Power and Propulsion Conference*. Beijing, China.

Nezhadali, V. and Eriksson, L. (2014). *Optimal lifting and path profile for a wheel loader considering engine and turbo limitations*. Optimization and Optimal Control in Automotive Systems, In Lecture Notes in Control Sciences, Editors: L. del Re, I. Kolmanovsky, M. Steinbuch and H. Waschl. Springer.

Nezhadali, V., Eriksson, L., and Fröberg, A. (2013). Modeling and optimal control of a wheel loader in the lift-transport section of the short loading cycle. In *AAC'13 – 7th IFAC Symposium on Advances in Automotive Control*. Tokyo, Japan.

Nilsson, T., Fröberg, A., and Åslund, J. (2013). Fuel and time minimization in a CVT wheel loader application. In *AAC'13 – 7th IFAC Symposium on Advances in Automotive Control*. Tokyo, Japan.

Sager, S. (2009). Reformulations and algorithms for the optimization of switching decisions in nonlinear optimal control. *Journal of Process Control*, 1238–1247.

Sarata, S., Weeramhaeng, Y., and Tsubouchi, T. (2005). Approach path generation to scooping position for wheel loader. In *IEEE International Conference on Robotics and Automation*. Barcelona, Spain.

Sivertsson, M. and Eriksson, L. (2013). Optimal transient control and effects of a small energy storage for a diesel-electric powertrain. In *AAC'13 – 7th IFAC Symposium on Advances in Automotive Control*. Tokyo, Japan.

TOMLAB (2012). PROPT - Matlab Optimal Control Software, "`http://www.tomdyn.com/`".

Volvo (2012). L220G wheel loader product brochure, "`http://www.volvoce.com/constructionequipment/na/en-us/products/wheelloaders/wheelloaders/L220G/Pages/specifications.aspx`".